Earthquakes and Structures, *Vol. 11, No. 4 (2016) 723-740*
DOI: http://dx.doi.org/10.12989/eas.2016.11.4.723

Shear strength model for reinforced concrete corbels based on panel response

Leonardo M. Massone* and Julio E. Álvarez[a]

Department of Civil Engineering, University of Chile, Blanco Encalada 2002, Santiago, Chile

(Received February 1, 2016, Revised October 10, 2016, Accepted October 11, 2016)

Abstract. Reinforced concrete corbels are generally used to transfer loads within a structural system, such as buildings, bridges, and facilities in general. They commonly present low aspect ratio, requiring an accurate model for shear strength prediction in order to promote flexural behavior. The model described here, originally developed for walls, was adapted for corbels. The model is based on a reinforced concrete panel, described by constitutive laws for concrete and steel and applied in a fixed direction. Equilibrium in the orthogonal direction to the shearing force allows for the estimation of the shear stress versus strain response. The original model yielded conservative results with important scatter, thus various modifications were implemented in order to improve strength predictions: 1) recalibration of the strut (crack) direction, capturing the absence of transverse reinforcement and axial load in most corbels, 2) inclusion of main (boundary) reinforcement in the equilibrium equation, capturing its participation in the mechanism, and 3) decrease in aspect ratio by considering the width of the loading plate in the formulation. To analyze the behavior of the theoretical model, a database of 109 specimens available in the literature was collected. The model yielded an average model-to-test shear strength ratio of 0.98 and a coefficient of variation of 0.16, showing also that most test variables are well captured with the model, and providing better results than the original model. The model strength prediction is compared with other models in the literature, resulting in one of the most accurate estimates.

Keywords: corbels; panel model; strength; reinforced concrete; shear

1. Introduction

Reinforced concrete corbels are commonly extensions of walls or columns in buildings, bridges and other infrastructures, acting in cantilever subjected to point loads. As extensions of other members, their aspect ratio is usually small (close to 1). Usually this type of elements is designed to withstand the shear forces V_u applied through the supported beam, and sometimes they also resist the action of the tensile force N_u, which is mainly due to temperature changes, shrinkage and creep on main beam supported by the corbel (Fig. 1). Typically, the corbel reinforcement consists of the main steel, A_s, and horizontal stirrups, A_h (Fig. 1). In addition, there are auxiliary bars required to hold the rebar cage in place. It should be noted that generally no transverse

*Corresponding author, Ph. D., Associate Professor, E-mail: lmassone@ing.uchile.cl
[a]Former civil engineering student

Copyright © 2016 Techno-Press, Ltd.
http://www.techno-press.com/journals/eas&subpage=7 ISSN: 2092-7614 (Print), 2092-7622 (Online)

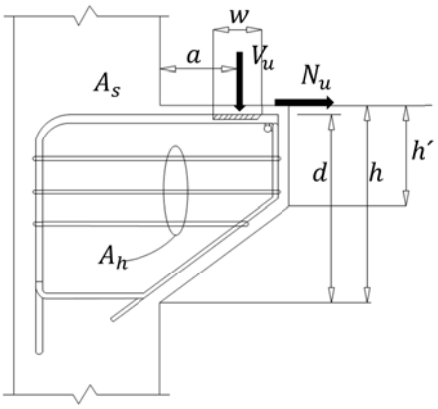

Fig. 1 Reinforced concrete corbels (after Russo *et al*. 2006)

reinforcement is used, which is considered less effective due to the steep incline of diagonal cracks.

Several models have been used to idealize the response of elements with low aspect ratio, such as squat walls, short beams, corbels, among others. The models with the largest complexities and accuracy are usually associated to finite element formulations. However, other models have also shown reasonable accuracy to predict shear strength with simpler formulations. There are empirical or semi-empirical models (i.e., Kriz and Raths 1965, Kumara and Barai 2010) that use main variables such as: secondary or web steel ratio (ρ_L), main or boundary steel ratio (ρ_b), concrete compressive strength (f'_c), aspect ratio (a/d), among others, and are calibrated to provide good predictions. Other models are based on strut and tie formulations (i.e., Solanki and Sabnis 1987, Russo *et al*. 2006, Kassem 2015) or a panel behavior that models the entire structural element. Some of these models are based on equilibrium, material constitutive laws and assumptions for compatibility, such that they do not only provide shear strength, but also provide the overall shear force versus shear displacement. Other models have included specific characteristics, such as the use of fiber in the concrete mix (i.e., Abdul-Razzak and Mohammed Ali 2011, Kumara and Barai 2010).

Within the first category, ACI 318-14 (2014) presents a method based on shear friction. This method assumes that both the main and secondary steel reinforcement crossing the shear plane are yielding. Failure occurs in a plane normal to the reinforcement on the inner side of the corbel. The aspect ratio is not explicitly included in the shear strength equations. The shear strength (V) of corbels is given by

$$V(\mathrm{N}) = \mu\left(\rho_f f_{yf} + \rho_h f_{yh}\right) bd \leq \left\{ \begin{matrix} 0.2\, f'_c bd \\ 11bd \\ (3.3 + 0.08\, f'_c)bd \end{matrix} \right\} \quad (1)$$

where μ is the coefficient of friction equal to 1.4 for monolithic concrete construction of normal weight; ρ_f is the main tensile reinforcement ratio; ρ_h is the secondary (web) reinforcement ratio; f'_c is the concrete compressive strength (MPa); f_{yf}, f_{yh} are the tensile yield stress for the main and secondary steel reinforcement, respectively (MPa); b is the width of the corbel (mm); d is the effective height of the corbel (mm).

The model by Solanki and Sabnis (1987) is based on a truss analogy with concrete resisting

only compression. Through equilibrium and from the geometry in the truss, the ratio of the horizontal distance of the applied shear force (a) to the effective height (d), a/d, is incorporated. The model for zero axial load yields to

$$V = \frac{\beta_1 b d f_c'}{4.45\sqrt{0.9^2+\left(\frac{a}{d}\right)^2}} \tag{2}$$

where β_1 is a parameter defined in ACI 318-14 (0.85 for low to normal concrete strength).

Kriz and Raths (1965) proposed a semi-empirical expression that includes the concrete compressive strength (f_c', MPa), the ratio a/d, as well as the main (A_s) and secondary (A_h) reinforcement. The model for zero axial load yields to

$$V = 0.54\, bd\, \sqrt{f_c'}\left(1 - 0.5\frac{d}{a}\right)(1000\rho)^{\frac{1}{3}} \tag{3}$$

where $\rho = \frac{A_S + A_v}{bd} \leq 0.02$ with $A_v < A_s$. Interestingly, the expression assumes that both main and secondary reinforcement are fully effective.

One of the modern models based on strut and tie formulation taking into account the contribution from concrete and secondary steel reinforcement ratio (ρ_h), is the one developed by Russo et al. (2006). Thus, the strut and tie model includes contribution of concrete strength (f_c'), that requires definition of the neutral axis depth ($kd = d\sqrt{\left(n\rho_f\right)^2 + 2n\rho_f} - n\rho_f$), which is based on equilibrium using the main reinforcement ratio (ρ_f), and the strut orientation ($\theta = 2\,\mathrm{atan}\left(\left(-1 + \sqrt{\left(\frac{a}{d}\right)^2 + \left(1 - \frac{k^2}{4}\right)}\right)\Big/\left(\frac{a}{d} - \frac{k}{2}\right)\right)$, rad) relative to the transverse direction, yielding to the strength (V)

$$V = c_1\left(k\,\chi\, f_c' \cos\theta + c_2\, \rho_h f_{yh} \cot\theta\right) bd \tag{4}$$

where $n = E_s/E_c = 42.6/\sqrt{f_c'}$ is the young modulus ratio (E_s is the steel modulus and E_c is the concrete modulus), b is the corbel width and d is the corbel effective length, f_{yh} is the secondary steel reinforcement yield strength (MPa) and $\chi = 0.74\left(\frac{f_c'}{105}\right)^3 - 1.28\left(\frac{f_c'}{105}\right)^2 + 0.22\left(\frac{f_c'}{105}\right) + 0.87$ is an interpolation function. The coefficients $c_1 = 0.8$ and $c_2 = 0.65$ are the values that better adjust the prediction of shear strength and scatter, respectively, for a database collected by Russo *et al.* (2006).

Many of these formulations have been originally developed to stablish shear strength of beams or short walls, and have been modified in order to predict the response of corbels. The category of panel or strut-and tie formulations are an example of this situation. The strut-and-tie model developed by Hwang *et al.* (2001) used the principles of equilibrium, compatibility and constitutive laws to estimate the shear strength for walls based on 3 trusses that involve the vertical and horizontal reinforcement and the main diagonal strut. Later, this model was adapted for corbels (Hwang *et al.* 2000a - later submittal than wall model) using most of the original assumptions.

The model, similar to others within this category, can only predict the shear strength. Panel models, in the other hand, assume uniform stress/strain fields within the entire wall section, which allows obtaining the shear force versus shear displacement response. In the work by Hsu and Mo (1985) compatibility is established for the entire wall, constitutive material laws are defined for concrete and steel, and equilibrium is determined in the longitudinal (vertical) direction, which

results in a nonlinear equation that requires solution for each displacement step. In order to solve the equilibrium equation the transverse normal strain (expansion) is considered equal to zero. This approach results in a principal stress/strain direction that rotates with the increment of lateral displacement (rotating-angle approach). Other similar proposed models have fixed the principal stress/strain direction (fixed-angle approach) to the geometric direction of the strut. A current research has shown that the cracking pattern might not be consistent with the direction of the main diagonal geometric direction (Kassem and Elsheikh 2010). The work by Kassem and Elsheikh calibrated expression for the principal strain/stress direction based on a best-fit analysis of shear strength estimate for a database of wall tests.

The model by Massone and Ulloa (2014) uses a similar methodology to the one developed by Kassem and Elsheikh, but determines the principal stress/strain direction differently. Two approaches were considered: (1) rotating-angle (crack) and (2) fixed-angle (crack) models, which are based on calibrated normal (vertical and horizontal) average strains for walls. The rotating-angle model uses directly the calibrated normal strains, since they are dependent on the shear distortion, which is assumed as the overall drift. Thus, upon estimation of the drift, the strain field is fully determined, defining the direction of the principal strain/stress angle. The fixed-angle approach, in the other hand, uses a similar procedure, but defines the strut direction upon reaching a prescribed tensile stress level in concrete, which is used for the entire analysis. In this case, the angle is calibrated based on different geometries, steel and concrete material properties. In the following sections, the model and the modifications applied for corbels is described. Only the fixed-angle case is analyzed which gives better and more consistent results.

The model described in this work is an adaptation and modification of the model developed by Massone and Ulloa (2014) for walls. The advantage of this type of models lays on its capability to capture not only strength, but also the overall shear load versus shear deformation of structures governed by shear. Moreover, since equilibrium, compatibility and constitutive material law are imposed; relevant features of the physical behavior are included. Thus, individual models that try to capture specific failure modes, which are ultimately related to material behavior (concrete, steel), such as shear friction do not require an especial treatment in this formulation. For example, the work by Hwang *et al*. (2000b) that studies the interface shear capacity (shear friction capacity), based on a strut and tie model, uses the same formulation as the work by Hwang *et al.* (2000a) for corbels, with an adaptation. Results revel that strength is correctly determined with better predictions than the shear friction equation of ACI 318 (2014).

2. Model formulation

The material model for reinforced concrete is based on the softened concrete compressive response under biaxial loading (cracking in the orthogonal direction) and the uniaxial behavior of steel, under the assumption of perfect adherence with concrete, as established by the modified compression field theory (MCFT) (Vecchio and Collins 1986).

2.1 Geometrical model

The analogy between short walls and corbels helps understanding how to apply the panel model for corbels. By rotating the corbel 90° and identifying the section that undergoes shear, that is, the

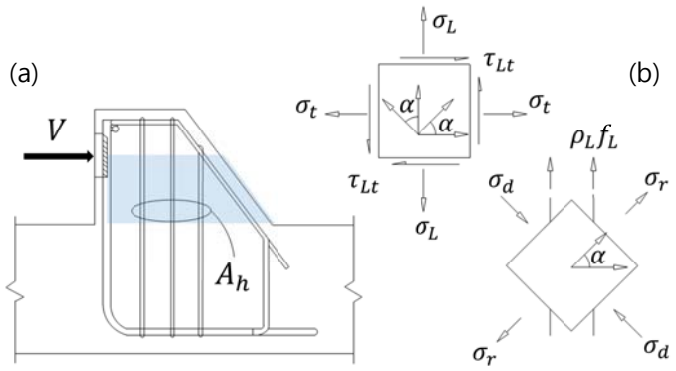

Fig. 2 Corbel configuration: (a) geometry (wall analogy), (b) concrete and steel stresses

section that emerges from the column with a point load at a height *a*, it is equivalent to a short wall in cantilever (Fig. 2(a)). Fig. 2(a) shows the vertical (main, A_s and secondary, A_h) reinforcement which is oriented in direction *L*. The reinforcement incorporated to hold the main and secondary reinforcement is not included in the model. The principal direction of concrete in compression goes along direction *d*, which is inclined at an angle α with respect to the longitudinal direction of the vertical reinforcement (Fig. 2(b)). The direction perpendicular to *d* is called *r* which is consistent with the principal tensile direction.

2.2 Equilibrium and compatibility

Assuming that web steel reinforcement is subjected to stresses along its longitudinal direction (no dowel action) and reinforcement is placed only in direction *L*; equilibrium equations that allow determining the shear force versus shear distortion are represented as follows

$$\sigma_L = \sigma_d cos^2\alpha + \sigma_r sin^2\alpha + \rho_L f_L = 0 \tag{5}$$

$$\tau_{Lt} = (-\sigma_d + \sigma_r) cos\alpha \, sin\alpha \tag{6}$$

where f_L is the average reinforcement stress in direction *L*, $\rho_L = \frac{A_h}{bd}$ is the secondary steel reinforcing ratio in the direction *L*, σ_L and σ_t are the average normal stress in the reinforced concrete panel in the respective directions, τ_{Lt} is the concrete shear stress in plane *L*-*t*, and finally, σ_d and σ_r are the principal concrete stresses in the principal directions *d* and *r* (Fig. 2(b)). In Eq. (5), only corbels without resultant load in direction *L* are considered (Fig. 2(a)).

Under uniform stress distribution, the shear resultant force is expressed as

$$V = \tau_{Lt} bd \tag{7}$$

where b is the corbel thickness and d is the corbel effective length (distance between main reinforcement and most compressive fiber, Fig. 2(a)). Compatibility is established for the entire panel section, assuming that stress and strain field principal directions coincide, yielding

$$\varepsilon_L = \varepsilon_d cos^2\alpha + \varepsilon_r sin^2\alpha \tag{8}$$

$$\varepsilon_t = \varepsilon_d sin^2\alpha + \varepsilon_r cos^2\alpha \tag{9}$$

$$\gamma_{Lt} = 2(\varepsilon_r - \varepsilon_d)cos\alpha\ sin\alpha \tag{10}$$

where $\varepsilon_L, \varepsilon_t, \varepsilon_d$ and ε_r are the normal strain values consistent with directions L, t, d and r, respectively, and γ_{Lt} is the shear strain in the L-t plane. The displacement consistent with V, when governed by the shear strain, is determined as

$$\Delta = \gamma_{Lt} a \tag{11}$$

where a is the height to the point load (Fig. 1(a)).

2.3 Material constitutive laws

2.3.1 Concrete

The material properties are identical as incorporated by Kassem and Elsheikh (2010) and Massone and Ulloa (2014). The constitutive law for concrete in compression is proposed by Zhang and Hsu (1998), which considers concrete compressive softening (d, direction) due to tensile strain (r, direction). The compressive (σ_d, negative for compression) response is described as

$$\sigma_d = -\zeta f'_c \left[2\left(\frac{-\varepsilon_d}{\zeta\varepsilon_0}\right) - \left(\frac{-\varepsilon_d}{\zeta\varepsilon_0}\right)^2\right],\ if\ \varepsilon_d \le \zeta\varepsilon_0 \tag{12}$$

$$\sigma_d = -\zeta f'_c \left[1 - \left(\frac{\frac{-\varepsilon_d}{\zeta\varepsilon_0} - 1}{\frac{2}{\zeta} - 1}\right)^2\right],\ if\ \varepsilon_d > \zeta\varepsilon_0 \tag{13}$$

$$\zeta = \frac{5.8}{\sqrt{f'_c}} \frac{1}{\sqrt{1+400\varepsilon_r}} \le \frac{0.9}{\sqrt{1+400\varepsilon_r}} \tag{14}$$

where ε_0 is the compressive strain consistent with f'_c (solid line, Fig. 3(a)), ζ is the reduction factor due to cracking (Fig. 3(a)) that causes softening in the compressive direction. Concrete in tension (σ_r, positive for tension) is modeled according to the work by Gupta and Rangan (1998) as

$$\sigma_r = E_c \varepsilon_r,\ if\ 0 \le \varepsilon_r \le \varepsilon_{ct} \tag{15}$$

$$\sigma_r = f'_{ct} \frac{(\varepsilon_{ut} - \varepsilon_r)}{(\varepsilon_{ut} - \varepsilon_{ct})},\ if\ \varepsilon_{ct} < \varepsilon_r \le \varepsilon_{ut} \tag{16}$$

$$\sigma_r = 0,\ if\ \varepsilon_{ut} < \varepsilon_r \tag{17}$$

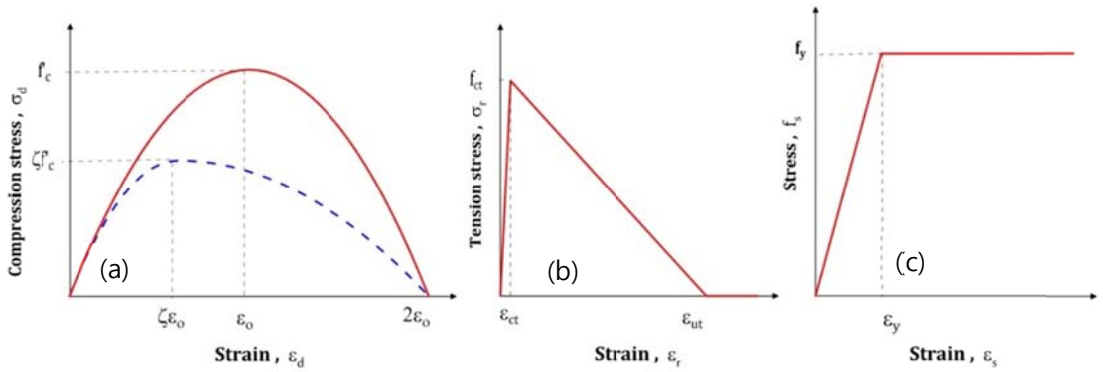

Fig. 3 Material constitutive laws: (a) concrete in compression, (b) concrete in tension, and (c) steel. (after Massone and Ulloa 2014)

where $f'_{ct} = 0.4\sqrt{f'_c(MPa)}$ is the tensile concrete strength with $\varepsilon_{ct} = f'_{ct}/E_c$ and $E_c = 4700\sqrt{f'_c(MPa)}$. Ultimate tensile strain, ε_{ut}, is set as 0.002 (Fig. 3(b)).

2.3.2 Reinforcing steel

The uniaxial model for reinforcing steel uses an elasto-plastic stress (f_s) versus strain (ε_s) response (Fig. 3(c)), defined as

$$f_s = E_s\varepsilon_s, \ \ if\ \varepsilon_s < \varepsilon_y \tag{18}$$

$$f_s = f_y, \ \ if\ \varepsilon_s \geq \varepsilon_y \tag{19}$$

where E_s is the steel reinforcement elastic modulus, f_y is the yield stress of steel.

2.4 Strain field

Different assumptions have been used by previous researchers to estimate the principal stress/strain angle (α). For walls, some of them have simply forced it to the direction of the geometric main diagonal. In the work by Kassem and Elsheikh (2010) the angle was calibrated to better capture the shear strength in walls. The work by Massone and Ulloa (2014) calibrated an angle for the fixed-angle model based on expressions for the average wall expansion (average transverse strain) and average wall vertical normal strains (Massone 2010). According to the study (Massone, 2010; Massone and Ulloa, 2014), the average (over the height) expansion (ε_t) and vertical average normal strain (ε_L) for the case with zero axial load and zero transverse reinforcement for walls with free-end condition (cantilever) reduces to

$$\varepsilon_t = 0.007(100\delta)^{1.4} \tag{20}$$

$$\varepsilon_L = 0.0073\left(\frac{a}{h} + 0.5\right)^{-0.37}(100\delta)^{0.93} \tag{21}$$

where $\delta = \Delta/a$ is the wall lateral top drift, and h is the entire length of the corbel.

The previous expressions for the wall transverse (ε_t) and longitudinal (ε_L) average normal strain values together with the drift level (assumed as the shear strain, γ_{Lt}), provides the full components of the strain field. The principal strain direction is determined by combining Eqs. (8), (9) and (10), yielding $\alpha = tan^{-1}\left(-\frac{(\varepsilon_t-\varepsilon_L)}{\gamma_{Lt}} + \sqrt{\left(\frac{\varepsilon_t-\varepsilon_L}{\gamma_{Lt}}\right)^2 + 1}\right)$, which changes (rotates) with the variation of strain values. A fixed-angle model assumes that the principal strain (and stress in most cases) direction remains unchanged with loading. For small wall top displacements, cracks have not formed yet, such that a main strut is not defined. Upon increments of drift levels, the principal tensile strain increases until the concrete tensile stress is reached $\sigma_r = f_{ct}$ (initiation of cracking). Further tensile straining reduces the tensile stress in concrete. Massone and Ulloa (2014) established two criteria: (1) $\sigma_r = f_{ct}$ (consistent with $\varepsilon_r = \varepsilon_{ct}$), and (2) $\sigma_r = 0.5f_{ct}$ (consistent with $\varepsilon_r = 0.5(\varepsilon_{ct} + \varepsilon_{ut})$). For this study, only the first criterion ($\sigma_r = f_{ct}$) is considered, such that the model is independent of the post-cracking formulation.

A wide variety of geometric properties (aspect ratio), axial load level, steel reinforcing ratio and material properties were used, based on the experimental database for walls collected by Massone and Ulloa (2014), in order to determine the crack direction. Least-square method was used to determine a calibrated expression for the crack direction. This consideration, although for an important range of parameters, the values are not necessary consistent the case of corbels. In this

study corbels without axial load (N) and transverse reinforcement are modeled, and therefore, the calibration for walls might not be adequate. The expression calibrated for cantilever walls, yielded,

$$\alpha = 175.2\left(\frac{a}{h}+5\right)^{-0.605}\left(\frac{N}{f'_c bh}+1\right)^{-4.6} \quad (22)$$

The principal strain and stress direction (α) is fixed for the entire analysis. Different drift levels are defined in order to obtain the overall shear load versus shear displacement based on compatibility (Eqs. (8)-(10)), material constitutive laws (Eqs. (12)-(19)) and longitudinal equilibrium (Eq. (5)), which establishes an iterative scheme. The equilibrium equation might be solved using Newton-Rapson. The shear force is determined with (Eqs. (6), (7)).

3. Model response

3.1 Experimental database

The database consists of 109 tests available in the literature, where the considered corbels were constructed symmetrically with respect to the column from where the corbels emerge. All specimens lack of transverse reinforcement, and 51% of the tests have no secondary reinforcement in the web. All corbels in the database were tested in the absence of axial load. For the preparation of the database, corbels with rectangular and variable cross-section are considered, respecting the recommendation and Kriz and Raths (1965) that limits the depth of the outer face of the corbel *h'* to at least half the depth of the inner face *h* to prevent premature failure at a plane outside the connection of the corbel base with the column, where the section varies. Specimens that presented failure due to detailing problems (such as failure at the load plate) were also excluded. The selected corbels have different configurations of reinforcement arrangement, *a/d* ratio, and material properties. The longitudinal secondary reinforcement ratio goes from 0% to 1.61%, with an average value of 0.35%, the main longitudinal reinforcement ratio ranges from 0.29% to 4.93%, with an average value of 1.28%. The ratio *a/d* ranges from 0.15 to 1.01, with an average value of 0.49. Although experimental tests with larger ratio *a/d* exist (i.e., Lu, Lin and Hwang, 2009), they are not selected, since those are less prone to shear failure. Yield stress of steel main longitudinal reinforcement varies between 303 (MPa) to 558 (MPa), with an average value of 380 (MPa). Similar values are observed for the longitudinal secondary reinforcement. The compressive strength of concrete ranges from 15 (MPa) to 105 (MPa), with 48 specimens over 40 (MPa) and an average value of 43 (MPa).

The database is collected from the information reported by Kriz and Raths (1965), Hermansen and Cowan (1974), Mattock *et al*. (1976), Fattuhi and Hughes (1989), Her (1990), Yong and Balaguru (1994), Fattuhi (1994), and Foster et al. (1996).

3.2 Original model - strength

In order to determine the shear strength for the entire database, the model was run for a large range of drift levels in order to observe the peak shear force. In the other hand, for the flexural capacity of the corbels, a simple flexural model was implemented based on sectional analysis using the same constitutive law for concrete and reinforcing steel, but without the concrete softening ($\zeta = 1$). Thus, failure type, based on shear and flexural capacity estimates, would be

associated to each specimen. Although for shear failure the entire shear force versus shear displacement (or strain) can be determined, the described database present limited information on overall response (such as load versus displacement). In the few cases, where the backbone curves are presented, the displacement is not just shear, but it also includes flexural deformation and it is probably also combined with strain penetration, among others. Therefore, only strength is compared in these sections, to avoid biased analysis. Comparison of shear force versus shear displacement has been presented in the original formulation (where the tests provided the required information) showing consistent results (Massone and Ulloa 2014).

The average ratio between the predicted capacity and the experimental value (V_{model}/V_{test}) for the entire database is 0.77, together with a coefficient of variation (COV) of 0.23. The capacity ratio reduces slightly to 0.75 for the cases that fail in shear (99 out of 109 specimens) with the same COV.

3.3 Model modifications

3.3.1 Effect of loading plate

Massone *et al*. (2013) determined that the profile of transverse strains develops along the shearing area with a shorter shear length than a. Experimental evidence showed that the strain expansion of beams is limited under the loading plates and supports. This is because including a plate (load point or support) prevents or interrupts the lateral expansion of the beam, favoring a shear crack between the plates. The expansion model (ε_x, Fig. 4) assumes that in the end this value is zero (Kang *et al*. 2012). In this formulation the expansion model is used to calibrate an expression for the location of the compression strut. Thus, this amendment applies only in determining the angle α. A decrease in the length a' will increase the capacity in the model due to the increment of the angle α.

This effect is included by defining the length *a'*, where the expansion is effective and it is used to determine the angle of the compressive strut. Thus, for a plate of width w, yields

$$a' = a - \frac{w}{2} \tag{23}$$

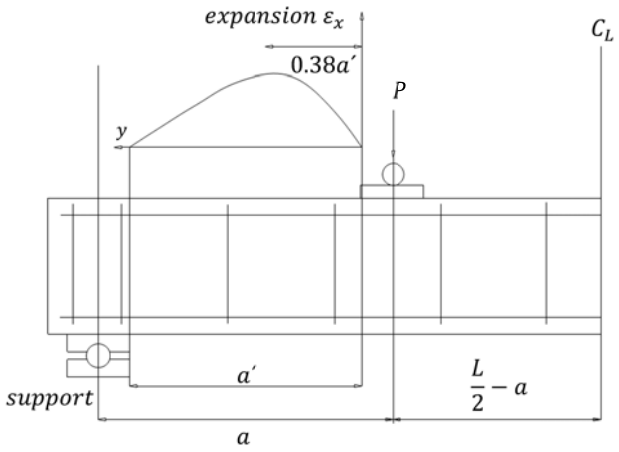

Fig. 4 Effect of the loading plate - distribution of expansion (after Kang *et al*. 2012)

In the case of the work by Fattuhi and Hughes (1989), and Fattuhi (1994) there is no information on the length of the loading plate, so that a length of 50 (mm) is assumed as it is done by Canha *et al*. (2014).

3.3.2 Effect of the main longitudinal reinforcement

The model by Massone and Ulloa (2014) incorporated into the formulation just the longitudinal web reinforcement in the equilibrium equation for short walls, without any contribution from the boundary reinforcement. In this case, the boundary reinforcement for walls corresponds to the main longitudinal reinforcement. Fig. 5 shows the trend of the ratio between the predicted capacity and the experimental value (V_{model}/V_{test}) to changes in the main longitudinal reinforcement ratio, incorporated as the available tensile panel stress given by such reinforcement ($\rho_b f_{yb}$, with $\rho_b = \frac{A_s}{bd}$ and f_{yb}, the yield stress of main reinforcement). The negative slope for the linear trend in the figure indicates that the capacity tends to be more conservatively estimated for larger available contribution from the main reinforcement. That is, if the capacity (for example, though equilibrium equation) has a dependency to the tensile capacity of the main reinforcement, the trend could be horizontal.

Experimental evidence by Kriz and Raths (1965) supports the inclusion of the main reinforcement in the shear strength in corbels. The authors conclude that the secondary steel (web) is as effective as the main reinforcement in corbels, which is explicitly shown in their empirical formulation (Eq. (3)).

The main reinforcement in terms of tensile panel stress given by such reinforcement ($\rho_b f_b$) for a tensile stress f_b, if assumed acting in a similar way as the secondary reinforcement, can be incorporated in the equilibrium equation for the normal longitudinal direction with an efficiency parameter β $(0 \leq \beta \leq 1)$, as

$$\sigma_L = \sigma_d \cos^2 \alpha + \sigma_r \sin^2 \alpha + \rho_L f_L + \beta \rho_b f_b \tag{24}$$

In order to incorporate the main reinforcement in the equilibrium equation, the same constitutive material law for the secondary steel is used with the consistent yield stress, but the

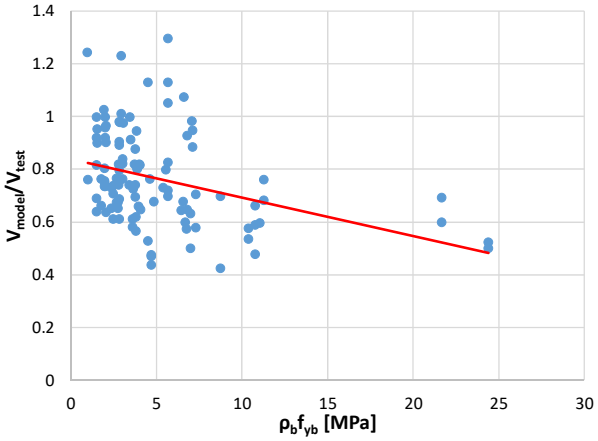

Fig. 5 Effect of the main reinforcement - original model

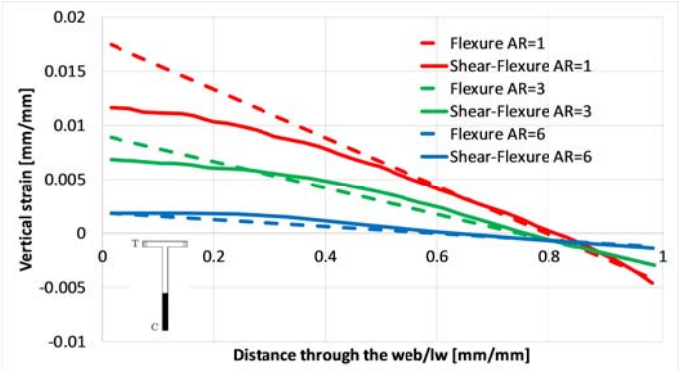

Fig. 6 Vertical profile of walls for different aspect ratio at a drift level of 0.5% (unpublished - after Hernández 2015)

longitudinal strain is required. Thus, knowing the strain on the main reinforcement completes the strain field. Little information is available providing this information. The work by Hernández (2015) on finite element analysis for T-shaped walls, indicate that cantilevered elements with a point lateral load (similar to the case of corbels under study) present variation of vertical strain long the length of the element that deviates from the Bernoulli hypothesis (plane sections remain plain after application of the load) as the aspect ratio reduces. Fig. 6 shows the strain profile along the length of the analyzed elements for 3 different aspect ratio (AR=1, 3 and 6) at 0.5% drift for 2 model formulations: (1) full finite element formulation (flexure-shear, FEM formulation), and (2) formulation imposing the Bernoulli hypothesis (flexure). Identical models were used for the two implementation, but in order to impose Bernoulli hypothesis, stiff horizontal elements were placed at each level resulting in a model that only incorporates flexure as same as a fiber model. As it can be seen, and as expected, the shorter the aspect ratio, the more that the tensile strain at the location of the boundary (main) reinforcement for the FEM formulation deviates from the case of pure flexure (Bernoulli hypothesis). Moreover, the tensile strain at the boundary (main) reinforcement tends to be similar to the strain at the center of the longitudinal web (secondary) reinforcement. In the case of corbels that usually present aspect ratio or *a/d* ratio lower than 1, it is reasonable to assume, as an approximation, that the strain of the main reinforcement (ε_b) coincide with the strain of the secondary reinforcement (ε_L), that is $\varepsilon_b = \varepsilon_L$.

The main reinforcement efficiency parameter β is calibrated ranging its value from 0 to 1 such that the COV is minimized for the specimens that fail under shear (controled in shear compared to the flexural capacity). The incorporation of the main reinforcement in the equilibrium equation (Eq. (24)) increases the capacity of the corbel, which should improve the accuracy of the model.

3.3.3 Effect of the strut direction (α) for corbels

As it was indicated in the formulation, the strain field is determined based on an estimate of the direction of the principal strain/stress direction (α). The calibration for α by Massone and Ulloa (2014) was based on expressions for vertical and horizontal average strain that are dependent on geometry, material properties, steel quantities, axial load and drift level. The calibration used a range for the parameters that were consistent with wall specimens, including the axial load and transversal reinforcement among others. In the case of corbels and for this study, the absence of axial load and transverse reinforcement suggests that the original calibration for α might not be

accurate. Thus, the procedure described in section 2.4 (strain field) is carried out, but for the corbel condition using Eqs. (20) and (21). As it can be expected, the calibrated expression would be dependent only on the *a/d* ratio. The strut direction for corbel yields

$$\alpha = 66.5\left(\frac{a}{h} + 5\right)^{-0.094} \tag{25}$$

Eqs. (22) and (25) for zero axial load fall apart by an almost constant angle of 5°, with Eq. (25) presenting a larger angle when ranging *a/d* between 0.1 and 1. The angle α in Eq. (25), varies from approximately 70° to 64°, respectively. A larger strut direction also results in an increase of the shear capacity for corbels.

3.4 Model modifications - strength

This section describes the results obtained when comparing the collected database with the model that includes all three modifications described in the previous sections: (1) effect of the loading plate, (2) effect of the main longitudinal reinforcement, and (3) effect of the strut direction for corbels. All of these modifications were incorporated in the model developed by Massone and Ulloa (2014) for the case where the formation of the strut direction is fixed once the tensile strength of concrete is reached ($\sigma_r = f_{ct}$, consistent with $\varepsilon_r = \varepsilon_{ct}$). All three new considerations are fully defined, except for the effect of the main longitudinal reinforcement due to the presence of the efficiency parameter β which can vary from 0 to 1. The model is run for the entire database varying parameter with increments of 0.1 and including all proposed modifications simultaneously.

Fig. 7 shows the results obtained for the average and coefficient of variation (COV) for the ratio between the predicted capacity and the experimental value (V_{model}/V_{test}) for all specimens and the group of specimens that fail in shear or flexure. As it can be seen in the figure, a value of $\beta = 0.3$ results in a minimum COV for the entire database and the cases that fail in shear. Such value is selected for further analysis.

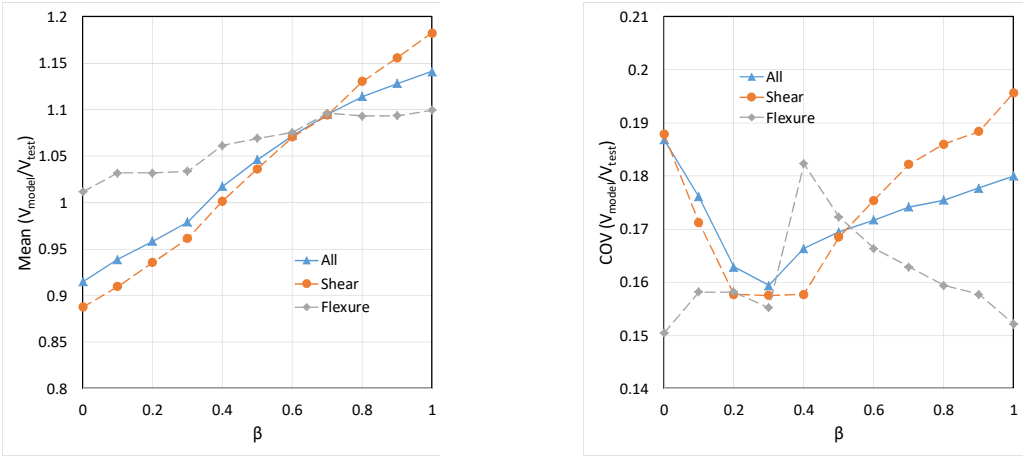

(a) (b)

Fig. 7 Statistical analysis of the model including all modifications for variations of the main reinforcement efficiency parameter (β) - V_{model}/V_{test} (a) average ratio, and (b) coefficient of variation (COV)

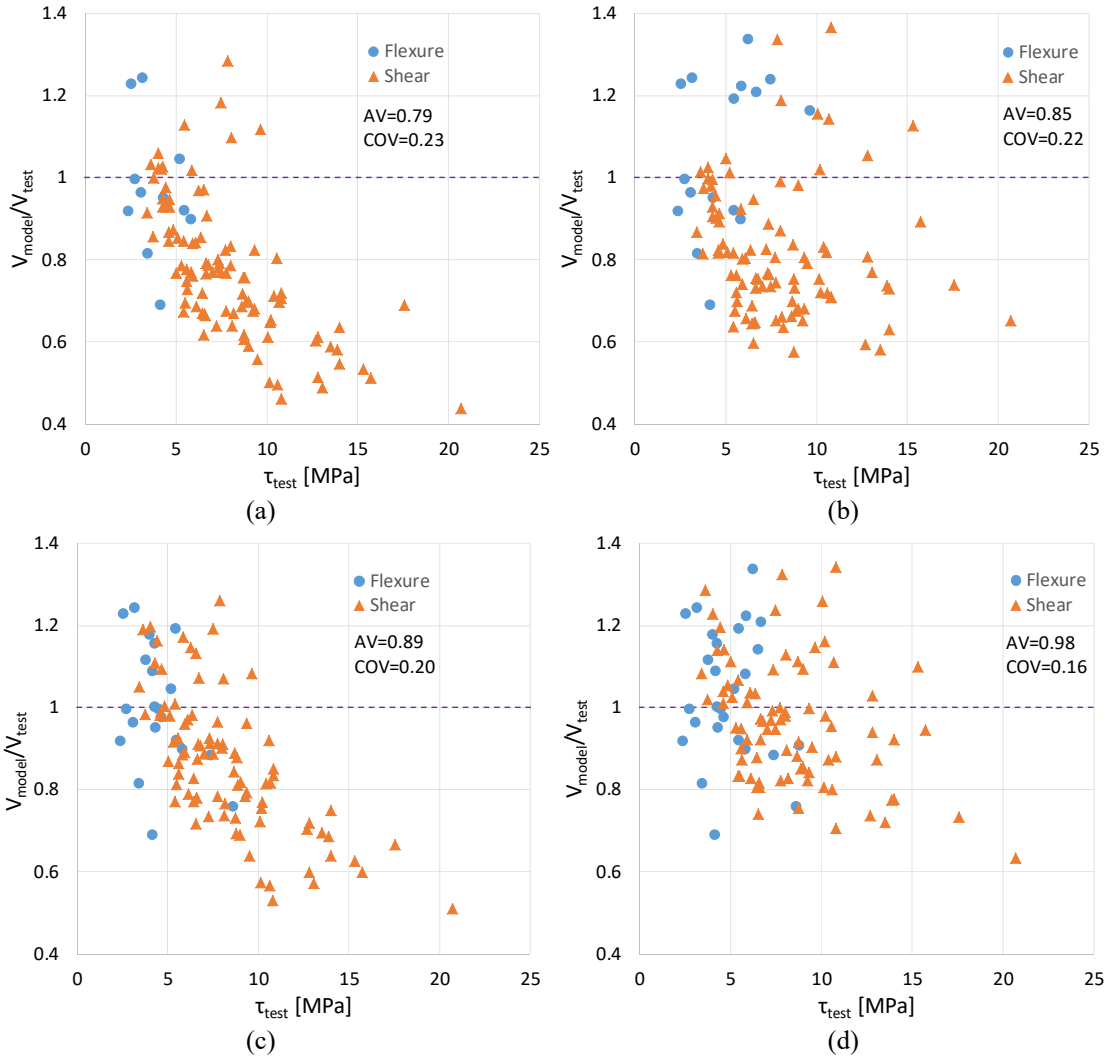

Fig. 8 Analysis of the model including different modifications (V_{model}/V_{test}) - (a) effect of the plate, (b) effect of the main reinforcement, (c) effect of the strut direction and (d) all modifications

In order to disaggregate the influence of each modification, the model is also run including the proposed modifications, but once a time. Fig. 8 shows the ratio between the predicted capacity and the experimental value (V_{model}/V_{test}, distinguishing between flexure and shear controlled) for all cases against the observed strength, as well as the average and COV separated in graphs that include 1 modification and all modifications simultaneously. As mentioned earlier, before the application of the modifications the model yields results of average strength ratio of 0.77 and COV of 0.23. The figure shows that the best results occurs for the case with all modifications included simultaneously (better average and less COV), with a strength ratio (V_{model}/V_{test}) of 0.98 and a COV of 0.16 for all specimens. Similar values are obtained for shear and flexure predicted failure (average of 0.96 and 1.03, and COV of 0.15 and 0.16, respectively for shear and flexure), which indicate that both models are capable of distinguishing the failure that controls them and their

capacity. In general, the models that do not include the effect of the main reinforcement tend to underestimate the shear strength with larger measured maximum shear stress. The larger the stress, the larger the conservatism. The incorporation of the main reinforcement corrects such situation maintaining a similar level of accuracy for all range of shear stress levels.

3.5 Model modifications - parameter sensitivity to strength

This section studies how the strength predictions are sensitive to different corbel parameters such as: aspect ratio *a/d*, secondary steel reinforcing ratio ($\rho_L f_{yL}$), main steel reinforcing ratio ($\rho_b f_{yb}$), and inner to outer corbel height ratio (h'/h) as shown in Fig. 9. All plots (Fig. 9) show the strength ratio between the model estimate and the experimental value (V_{model}/V_{test}) versus the parameter under analysis for the model (including all modifications).

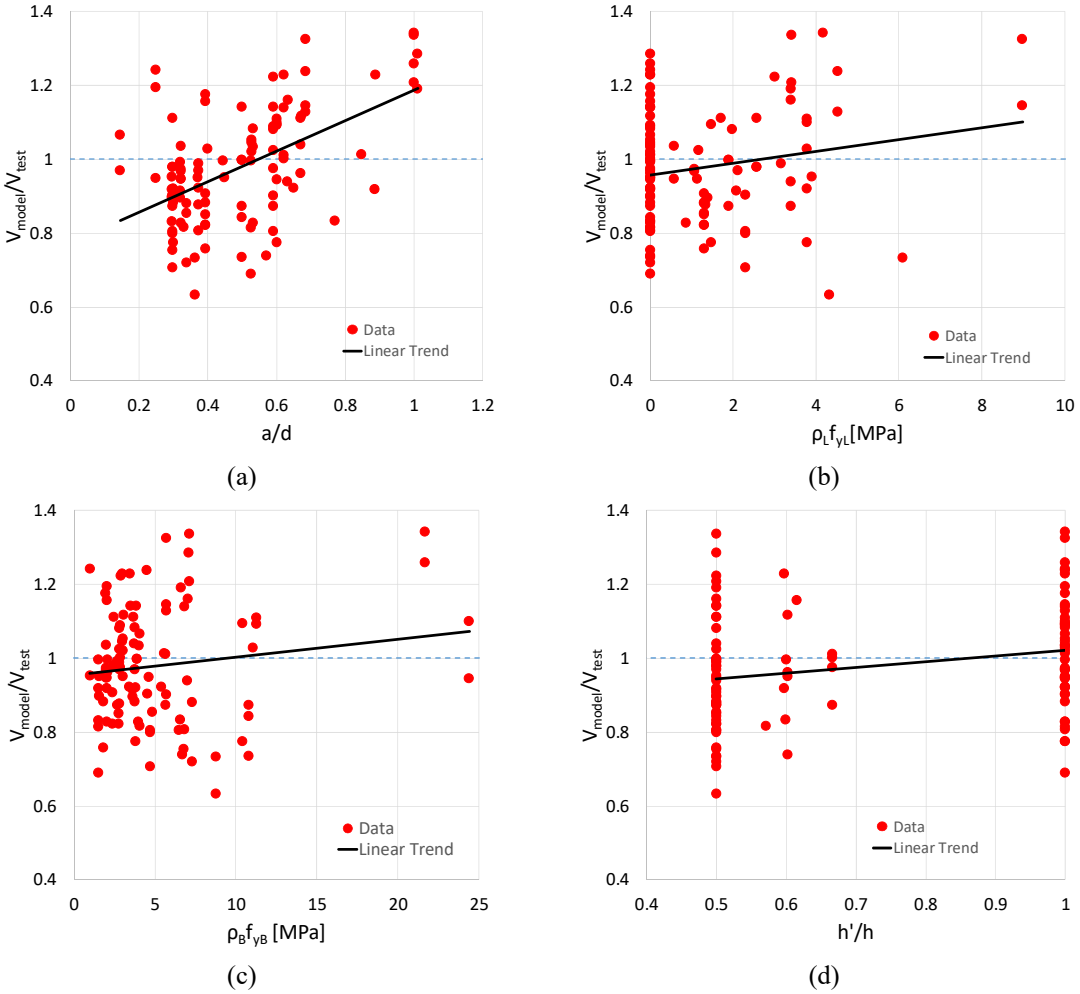

Fig. 9 Sensitivity of average strength ratio (V_{model}/V_{test}) to - (a) aspect ratio (*a/d*), (b) secondary steel strength ratio ($\rho_L f_{yL}$), (c) main steel strength ratio ($\rho_b f_{yb}$), and (d) inner to outer height ratio (h'/h)

As it can be seen in the figure, from all parameters, there is little dependency to the secondary steel reinforcing ratio, main steel reinforcing ratio and inner to outer corbel height ratio with average strength ratio variation generally less than 20% for the range of test data, which indicates that the model is capable of capturing the influence of these variables to estimate the shear strength. It is important to highlight that in the case of the main reinforcement (Fig. 9(c)), that presents a trend line that moves relatively close to the value of 1, before the modifications showed a completely different behavior. In Fig. 5, not only the model results for the original formulation (without modifications) were more conservative, but also indicate a dependency (average strength ratio variation close to 40% for the range of test data) to the main reinforcement ratio, that is almost inexistent once it is incorporated in the equilibrium equation (Fig. 9(c)). That indicates that the main reinforcement effect is well captured by the modified model.

According to Fig. 9(a), the model presents moderate dependency to the aspect ratio, with average strength ratio variation close to 40%, approximately, for the range of test data. Almost all models have trend lines under the strength ratio of 1.0. As the aspect ratio increases, the behavior is more flexural, which might indicate that the model used to estimate the flexural capacity could be improved in order to better capture its dependency.

Fig. 9(d) shows that the inner to outer corbel height ratio (corbels with rectangular or variable section) has no dependency to the strength ratio. This parameter is not included in the formulation, which indicates that such consideration is correct. However, it is important to point out that the database was collected maintaining the recommendation by Kriz and Raths (1965) that suggests $h'/h \geq 0.5$ to avoid an undesearable failure mode.

3.6 Comparison to other models - strength

In this section, different models from the literature are considered for comparison with the proposed formulation including all modifications. The models were described in the introduction and goes from shear friction models (ACI 318-14, 2014) in Eq. (1) to empirical or semi-empirical expressions based on concepts of strut-and-tie models, such as the model by Solanki and Sabnis (1987) in Eq. (2), Kriz and Raths (1965) in Eq. (3) and Russo *et al*. (2006) in Eq. (4). The shear strength is calculated based on the described expressions, along with the estimation of the flexural capacity described in this work.

In order to include all requirements incorporated in the models used for the comparison, a subset of the database is used for the analysis. The limitations stipulated by the models are such that they comply with the minimum reinforcement by ACI 318-14, defined as $\rho_b = 0.04 f_c^{'} / f_y$, and also the requirement imposed by Kriz and Raths (1965), where only corbels with a total steel ratio less than 2% and with larger amount of the secondary (web) steel reinforcement than the main reinforcement (boundary) are considered. This results in a database with 68 specimens.

In Table 1, the main results are shown (average, standard deviation and COV for the model-to-test strength ratio). The shear friction model from ACI 318 (2014) presents the largest COV (0.24) with a conservative estimate of strength (0.84) for the entire database, whereas the model by Russo *et al*. (2006) and the proposed model provide the most accurate results with a strength ratio close to 1 and COV of 0.13. Low COV and strength ratio close to 1 for the cases that fail in flexure also indicate that the flexural behavior is also well captured. The semi-empirical model by Kriz and Raths (1965) presents also relatively good results, which is in part given that a portion of the database was used for the calibration of the formulation. The model by Solanki and Sabnis (1987) also correlates well with test results, however, these last two formulations lack on the inclusion of

Table 1 Comparison with models in the literature

Cases	$\frac{V_{model}}{V_{test}}$	ACI 318-14	Solanki and Sabnis	Kriz and Raths	Russo et al.	Original model	Proposed model
All	Avg	0.84	0.95	0.9	1.01	0.81	0.99
	SD	0.20	0.14	0.11	0.13	0.14	0.13
	COV	0.24	0.14	0.13	0.13	0.18	0.13
Shear	Avg	0.78	0.93	0.90	1.00	0.79	0.97
	SD	0.17	0.14	0.11	0.13	0.13	0.13
	COV	0.21	0.15	0.13	0.13	0.17	0.13
	No	53	51	64	54	62	51
Flexure	Avg	1.06	1.02	0.93	1.04	0.98	1.05
	SD	0.17	0.11	0.09	0.11	0.14	0.11
	COV	0.16	0.11	0.1	0.1	0.14	0.11
	No	15	17	4	14	6	17

the biaxial behavior of concrete and the absence of the yield stress of steel.

4. Conclusions

A simple fixed-angle model capable of predicting the shear load versus shear displacement response of reinforced concrete corbels under lateral loads is presented. The models use a panel formulation based on average stress and strain fields for a single reinforced concrete section, with coincident directions between the principal strain and stress concrete fields, and perfect adherence between concrete and steel. Concrete response is incorporated in the two principal directions with uniaxial material constitutive laws in tension and compression, including softening of concrete in compression. Steel reinforcement is represented with an elasto-plastic uniaxial model. The principal direction is fixed, whose direction is defined based on compatibility and a calibrated expression for normal strain variation with shear distortion at the initiation of cracking ($\sigma_r = f_{ct}$).

The formulation is based on the model by Massone and Ulloa (2014) developed for walls, which is adapted for corbels and modified in order to incorporate additional considerations that improve the shear capacity estimate and the dependency to several model parameters. The average of the ratio between the predicted capacity (before the modifications are applied to the model) and the experimental value (V_{model}/V_{test}) is 0.77 and the COV is 0.23 for a database collected from the literature with 109 specimens. Three modifications were applied to the model in order to improve the average and COV of the strength estimate. The modifications incorporated in the model were:

1) Effect of the loading plate: the presence of the loading plate reduces the length of the element that is capable of developing the expansion of the element, as it has been observed in beams. The modification results in a shorter length of the available height (a), which changes (increases) the strut direction increasing the shear capacity.

2) Effect of the main longitudinal reinforcement: The original equilibrium equation accounts for the presence of secondary reinforcement. Experimental evidence indicates that the main reinforcement also increases the shear capacity. Thus, the main reinforcement is incorporated in

the equilibrium equation, increasing the shear strength, with an efficiency factor, which was determined to be $\beta=0.3$ to minimize the COV for the database.

3) Effect of strut direction: the original formulation (Massone and Ulloa 2014) uses a strut direction that was calibrated based on normal strain expressions and analyzed for a range of values for parameters consistent with wall characteristics. For this study, corbels are analyzed without axial load and without transverse reinforcement. Re-calibration of the strut direction for parameters consistent with corbels results in an increase of about 5° for a/d in a range between 0.1 and 1. A larger strut angle increases the shear strength.

The incorporation of all three modifications resulted in good predictions with an average strength ratio of 0.98 and a COV of 0.16 for the entire database. The incorporation of each modification individually indicates that the effect of strut direction and the main reinforcement have a similar impact in strength prediction, presenting a smaller relevance the incorporation of the effect of the loading plate. The use of all modifications not only improves the strength estimate, but also shows that most parameters are well captured in the formulation when comparing the strength estimate with different parameters.

The model is also compared with expressions from the literature for a reduced database that is consistent with the restrictions imposed by the models. The results from the proposed model give similar accuracy as the model by Russo *et al.* (2006) and other models. However, the proposed model is also capable of determining the overall shear stress versus shear strain backbone curve, which is nowadays useful for performance-based design.

References

Abdul-Razzak, A.A. and Mohammed Ali, A.A. (2011), "Influence of cracked concrete models on the nonlinear analysis of High Strength Steel Fibre Reinforced Concrete corbels", *Compos. Struct.*, **93**(9), 2277-2287.

ACI Committee 318 (2014), "Building Code Requirements for Structural Concrete (ACI 318-14) and Commentary (318R-14)", *American Concrete Institute*, Farmington Hills, Mich.

Canha, R.M.F., Kuchma, D.A., El Debs, M.K. and Souza, R.A. (2014), "Numerical analysis of reinforced high strength concrete corbels", *Eng. Struct.*, **74**, 130-144.

Fattuhi, N.I. and Hughes, B.P. (1989), "Ductility of reinforced concrete corbels containing either steel fibers or stirrups", *ACI Struct. J.*, **86**(6), 644-651.

Fattuhi, N.I. (1994), "Reinforced corbels made with plain and fiber concretes", *ACI Struct. J.*, **91**(5), 530-536.

Foster, S.J., Powell, R.E. and Selim, H.S. (1996), "Performance of high-strength concrete corbels", *ACI Struct. J.*, **93**(5), 555-563.

Gupta, A. and Rangan, B.V. (1998), "High-strength concrete structural walls", *ACI Struct. J.*, **95**(2), 194-205.

Her, G.J. (1990), "Study of reinforced high-strength concrete corbels", Master's thesis, Department of Construction Engineering, *National Taiwan University of Science and Technology*, Taipei, Taiwan. (in Chinese)

Hermansen, B.R. and Cowan, J. (1974), "Modified shear-friction theory for bracket design", *ACI J., Proceedings*, **71**(2), 55-60.

Hernandez, A. (2015), "Verification of the Bernoulli hypothesis in combined reinforced concrete wall sections", *Civil engineering thesis*, Civil Engineering department, University of Chile. (in Spanish)

Hsu, T.T.C. and Mo, Y.L. (1985), "Softening of concrete in low-rise shearwalls", *ACI Struct. J.*, **82**(6), 883-889.

Hwang, S.J., Lu, W.Y. and Lee, H.J. (2000a), "Shear strength prediction for reinforced concrete corbels", *ACI Struct. J.*, **97**(4), 543-552.
Hwang, S.J., Yu, H.W. and Lee, H.J. (2000b), "Theory of interface shear capacity of reinforced concrete", *J. Struct. Eng.*, **126**(6), 700-707.
Hwang, S.J., Fang, W.H., Lee, H.J. and Yu, H.W. (2001), "Analytical model for predicting shear strength of squat walls", *J. Struct. Eng.*, **127**(1), 43-50.
Kang, T.H.-K., Kim, W., Massone, L.M. and Galleguillos, T.A. (2012), "Shear-flexure coupling behavior of steel fiber-reinforced concrete beams", *ACI Struct. J.*, **109**(4), 435-444.
Kassem, W. and Elsheikh, A. (2010), "Estimation of shear strength of structural shear walls", *J. Struct. Eng.*, **136**(10), 1215-1224.
Kassem, W. (2015), "Strength prediction of corbels using Strut-and-Tie model analysis", *Int. J. Concrete Struct. Mater.*, **9**(2), 255-266.
Kriz, L.B. and Raths, C.H. (1965), "Connections in precast concrete structures-strength of corbels", *PCI/ J.*, **10**(1), 16-61.
Kumara, S. and Barai, S.V. (2010), "Neural networks modeling of shear strength of SFRC corbels without stirrups", *Appl. Soft Comput.*, **10**(1), 135-148.
Lu, W.-Y., Lin, I.-J. and Hwang, S.-J. (2009), "Shear strength of reinforced concrete corbels", *Magaz. Concrete Res.*, **61**(10), 807-813.
Massone, L.M., Gotschlich, N.J., Kang T.H.-K. and Hong, S.-G. (2013), "Shear-flexural interaction for prestressed self-consolidating concrete beams", *Eng. Struct.*, **56**, 1464-1473.
Massone, L.M. (2010), "Strength prediction of squat structural walls via calibration of a shear-flexure interaction model", *Eng. Struct.*, **32**(4), 922-932.
Massone, L.M. and Ulloa, M.A. (2014), "Shear response estimate for squat reinforced concrete walls via a single panel model", *Earthq. Struct.*, **7**(5), 647-665.
Mattock, A.H., Chen, K.C. and Soongswang, K. (1976), "Behavior of reinforced concrete corbels", *PCI J.*, **21**(2), 52-77.
Russo, G., Venir, R., Pauletta, M. and Somma, G. (2006), "Reinforced concrete corbels shear strength model and design formula", *ACI Struct. J.*, **103**(1), 3-7.
Solanki, H. and Sabnis, G.M. (1987), "Reinforced concrete corbels-simplified", *ACI Struct. J.*, **84**(5), 428-432.
Vecchio, F. and Collins, M.P. (1986), "The modified compression-field theory for reinforced concrete elements subjected to shear", *ACI Struct. J.*, **83**(2), 219-231.
Yong, Y.K. and Balaguru, P. (1994), "Behavior of reinforced high-strength concrete corbels", *J. Struct. Eng.*, ASCE, **120**(4), 1182-1201.
Zhang, L.-X.B. and Hsu, T.T.C. (1998), "Behavior and analysis of 100 MPa concrete membrane elements", *J. Struct. Eng.*, **124**(1), 24-34.

CC